BMJ Open Respiratory Research

# Prognostic value of pulmonary vessel-related structures in rapid progression of idiopathic inflammatory myopathy-associated interstitial lung disease: a retrospective study from two centres

Yuhui Qiang ,[1,2] Hongyi Wang,[3] Xiaoyan Yang,[4] Yifei Ni,[3,5] Jianping Wang,[1,5] Anqi Liu,[3,5] Jie Du,[3,5] Linfeng Xi ,[1,2] Yinan Hu,[1,2] Yanhong Ren,[1,2] Bingbing Xie,[1,2] Shiyao Wang ,[1,2] Li Zhu,[6] Jing Geng,[1,2] Min Liu ,[5] Huaping Dai[1,2]

**To cite:** Qiang Y, Wang H, Yang X, *et al*. Prognostic value of pulmonary vessel-related structures in rapid progression of idiopathic inflammatory myopathy-associated interstitial lung disease: a retrospective study from two centres. *BMJ Open Respir Res* 2025;**12**:e003510. doi:10.1136/bmjresp-2025-003510

► Additional supplemental material is published online only. To view, please visit the journal online (https://doi.org/10.1136/bmjresp-2025-003510).

YQ, HW and XY are joint first authors.

Received 30 May 2025
Accepted 2 November 2025



For numbered affiliations see end of article.

**Correspondence to**
Dr Huaping Dai;
daihuaping@ccmu.edu.cn
and
Dr Min Liu;
mikie0763@126.com

## ABSTRACT

**Background** Pulmonary vessel-related structural (PVRS) abnormalities have been implicated in usual interstitial pneumonia; however, their significance in idiopathic inflammatory myopathy-associated interstitial lung disease (IIM-ILD) remains unclear. In this two-centre study, we evaluated the associations between PVRS parameters on high-resolution computed tomography (HRCT) and rapid progression and prognosis in patients with IIM-ILD.

**Methods** A total of 578 IIM-ILD patients (412 females; median age, 53 years) were included from retrospective ILD cohorts of two centres. Artificial intelligence (AI)-based quantification was performed on baseline HRCT to assess PVRS and interstitial lesions. The value of PVRS for rapid progression and prognosis was first evaluated in the cohort from the first centre using logistic regression, Kaplan-Meier analysis and Cox models. An independent cohort of 64 patients (43 female; median age, 54 years) from the second centre then served to validate the generalisability of the PVRS-based model of IIM-ILD progression.

**Results** In the first-centre cohort, 249 patients with rapidly progressive ILD (RP-ILD) showed significantly elevated mean pulmonary vascular diameter (mPVD) ($p<0.05$), shorter vascular-pleural distances, greater PVRS volume and higher standard deviation of pulmonary vascular diameter (sdPVD) ($p<0.001$) compared with non-RP-ILD patients. Multivariate analysis identified age (HR 1.03, 95% CI 1.01 to 1.06), ground glass opacity percentage (HR 1.04, 95% CI 1.02 to 1.06) and sdPVD at 6 mm and 18 mm from the pleura as independent risk factors for poor prognosis in antisynthetase syndrome (ASS) patients (concordance index (C-index)=0.819). In contrast, for patients with antimelanoma differentiation-associated gene 5 antibody-positive dermatomyositis (MDA5+DM), the independent risk factors were age (HR 1.06, 95% CI 1.02 to 1.11), mPVD at 6 mm from the pleura and lactic dehydrogenase levels (C-index=0.835). When applied to the external validation cohort, the respective multivariate Cox models yielded C-indices of 0.841 for ASS and 0.814 for MDA5+DM, confirming their generalisability.

**Conclusions** Our study demonstrates that baseline PVRS parameters on HRCT are robust imaging biomarkers associated with rapid progression and poor prognosis in IIM-ILD. These findings underscore the clinical relevance of PVRS assessment in risk stratification and management.

### WHAT IS ALREADY KNOWN ON THIS TOPIC

⇒ Prior studies have identified high interstitial lung disease (ILD) mortality in inflammatory myopathy (IIM) subtypes linked to vascular dysregulation, and quantitative CT metrics have been shown to aid disease assessment.

### WHAT THIS STUDY ADDS

⇒ This study provides evidence that pulmonary vessel-related structural parameters distinguish rapid from non-rapid progressors in IIM-ILD. It further establishes the clinical relevance of pleura-distance-specific mean pulmonary vascular diameter and standard deviation of pulmonary vascular diameter as quantitative biomarkers for stratifying disease severity in antimelanoma differentiation-associated gene 5 antibody-positive dermatomyositis (MDA5+DM) and antisynthetase syndrome (ASS)-ILD.

### HOW THIS STUDY MIGHT AFFECT RESEARCH, PRACTICE OR POLICY

⇒ In clinical practice, this study suggests that integrating CT-based PVRS parameters with standard clinical features provides a more nuanced approach to distinguish patients at varying risk levels. This strategy could significantly improve patient management by facilitating earlier and more personalised treatment decisions for patients with ASS and MDA5+DM.

## BACKGROUND

Interstitial lung disease (ILD) is a common and serious pulmonary complication of idiopathic inflammatory myopathies (IIM), particularly in patients with antisynthetase syndrome (ASS) or antimelanoma

differentiation-associated gene 5 antibody-positive dermatomyositis (MDA5+DM).[1–5] The severity is underscored by rapidly progressive ILD (RP-ILD), which occurs in approximately 80% of MDA5+DM cases and 7.8%–8.9% of ASS cases[6 7] and is associated with a 6-month mortality exceeding 50% due to acute respiratory failure.[8–10] This grave prognosis highlights the critical need for early prediction and timely, aggressive intervention to improve patient outcomes.

Emerging evidence indicates that dysregulated angiogenesis constitutes a critical pathophysiological mechanism underlying pulmonary fibrosis development.[11] Moreover, recent advancements in quantitative CT (QCT) analysis offer superior accuracy compared with visual assessments,[11–14] providing a robust framework for exploring correlations between imaging features and disease prognosis. QCT-derived pulmonary vessel-related structures (PVRS) have demonstrated utility in predicting usual interstitial pneumonia patterns and evaluating connective tissue disease-related ILD.[15–19] QCT-derived pulmonary vessel volume has demonstrated the strongest association with restrictive functional indices and could represent a new automated index of disease severity in hypersensitivity pneumonitis.[20] The integration of artificial intelligence (AI) now enables efficient, sophisticated QCT analysis. Leveraging this approach, our study specifically evaluates the association between AI-quantified PVRS characteristics of high-resolution computed tomography (HRCT) and disease progression trajectories in IIM-ILD.

## METHODS

### Study design and population

This retrospective cohort study of ILD was conducted in accordance with the ethical standards of the institutional ethics committee and the Declaration of Helsinki (1975, as revised in 2000). The institutional ethics committee of China-Japan Friendship Hospital approved the study protocol (No. KYLL-2019–455). The institutional ethics committee of General Hospital of Ningxia Medical University approved the study protocol on 16 March 2017 (No. 2017–25). Informed consent was obtained from all participants. The study included all patients diagnosed with ASS or MDA5+ DM-ILD between January 2016 and December 2021 at our hospital. Additionally, an independent external cohort from a second hospital, spanning January 2020 to December 2021, was recruited to validate the generalisability of the PVRS-based model for IIM-ILD progression. This external validation cohort was designed to further validate the findings and ensure the robustness of the study results.

All cases of IIM-ILD were diagnosed through a multidisciplinary discussion (MDD) involving specialists from pulmonary and critical care medicine, rheumatology, radiology and pathology. The diagnosis adhered to established criteria for IIM and ILD, with consensus reached by all MDD members.[9 21 22] Specifically, dermatomyositis (DM) was diagnosed according to the Bohan and Peter criteria and the 239th European Neuromuscular Centre International Workshop guidelines.[23 24] The diagnosis of ASS was confirmed by the presence of antiaminoacyl-transfer ribonucleic acid (tRNA) synthase antibodies and at least one of the triad findings: myositis, arthritis or ILD.[25] Serum autoantibodies (antiaminoacyl-tRNA synthase and anti-MDA5) were detected using commercial kits (EUROIMMUN, Lübeck, Germany) per the manufacturer's protocols.

The inclusion criteria were defined as: (1) age ≥18 years, (2) a confirmed diagnosis of ASS or MDA5+DM, and (3) availability of a baseline HRCT scan prior to initiation of treatment. Exclusion criteria comprised the absence of a baseline HRCT, poor image quality precluding analysis or incomplete clinical data leading to loss to follow-up. Figure 1 provides a flowchart outlining the participant selection process and group allocation.

### Clinical data

Demographics, clinical subtypes, treatment protocols and laboratory findings, including results from arterial blood gas analysis and inflammatory markers, were extracted from the ILD cohort and electronic medical records. All enrolled patients underwent standardised diagnostic evaluations at their initial presentation. Pulmonary function tests were performed (MasterScreen, Vyaire Medical GmbH, Hoechberg, Germany) within 1 week before or after the HRCT scan. Data were collected for pulmonary function parameters, including vital capacity (VC), forced vital capacity (FVC), forced expiratory volume in the first second ($FEV_1$), total lung capacity and single-breath carbon monoxide diffusing capacity ($DL_{CO}$ SB), along with their per cent predicted value.

Patients were classified into RP-ILD and non-RP-ILD based on clinical manifestations. In this study, the criteria for identifying RP-ILD were adapted from the international consensus statements modified by the American Thoracic Society (ATS) guidelines regarding idiopathic pulmonary fibrosis (IPF).[26 27] RP-ILD was defined when at least two of the following indicators occurred within 3 months of symptom onset: (1) worsening of respiratory symptoms, such as exertional dyspnoea; (2) increased pulmonary opacification on HRCT, including ground glass opacity (GGO), consolidation, reticular pattern or honeycombing; (3) physiological deterioration indicated by respiratory failure: defined as a >10% decrease in VC or a >1.33 kPa decrease in arterial oxygen tension ($PaO_2$). Non-RP-ILD was defined as disease that progresses gradually or remains stable beyond 3 months.

### HRCT scan

All patients underwent HRCT on multidetector CT systems (LightSpeed VCT/64, GE Healthcare; Toshiba Aquilion ONE TSX-301C/320; iCT/256 Philips; FLASH Dual Source CT, Siemens) in a single, breath-hold scan from the supine position. Acquisition and reconstruction

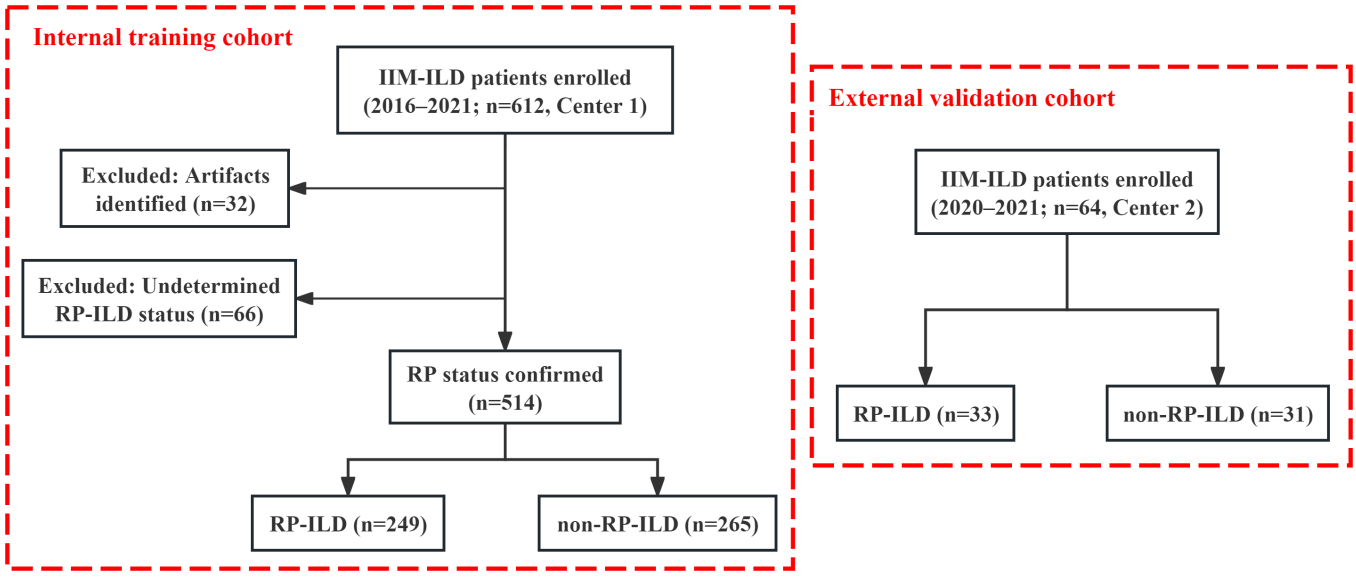


**Figure 1** Flow diagram of eligibility criteria. IIM-ILD, idiopathic inflammatory myopathy-related interstitial lung disease; RP-ILD, rapidly progressive interstitial lung disease; non-RP-ILD, non-rapidly progressive interstitial lung disease.

parameters followed standard CT protocols, including tube voltage of 100–120 kV, tube current of 100–300 mAs and slice thickness of 0.625–1 mm. Scanning table movement was set at 39.37 mm/s, with a gantry revolution rate of 0.8 s. Reconstruction was carried out progressively with slice thicknesses of up to 1 mm.

### AI-based quantitative CT analysis

HRCT images in the Digital Imaging and Communications in Medicine format were transferred to an in-house AI workstation (CT quantitative system: SIMBIO-T, Hangzhou Smart Intelligent Technology Hangzhou, China) for automatic quantitative analysis of lung parenchyma, pulmonary vessels, lung texture and radiomics parameters. The analysis pipeline consisted of two main phases (figure 2): (1) AI-based segmentation and quantification: the commercial AI algorithm was applied to automatically segment the entire lung, its lobes, pulmonary vessels and interstitial lesions and to calculate various quantitative features related to these structures. Prior to its use in this study, the performance of this algorithm was independently validated by our team on a subset of our dataset that was not included in the final analysis. Segmentation accuracy was assessed by quantifying the agreement between the AI output and manual annotations made by an expert radiologist using the Dice similarity coefficient, which was 0.95±0.02. The reproducibility of quantitative measurements was evaluated using the intraclass correlation coefficient, which was 0.92. (2) Radiologist review and adjudication: two chest radiologists with 9 and 15 years of experience independently evaluated all AI-generated segmentations using a standardised scoring system. Both radiologists were blinded to clinical information and to each other's assessments. Any discrepancies in the evaluations were resolved through a consensus discussion with a third senior chest radiologist with 22 years of experience.

### Statistical analysis

Statistical analyses were performed using IBM SPSS Statistics 26.0 (SPSS, MAC version, IBM, Armonk, USA) and R (V.4.4.1, R Foundation for Statistical Computing, Vienna, Austria). The normality of the distribution for continuous characteristics was assessed using the Kolmogorov-Smirnov test. T-tests were used to compare variables that were normally distributed, and these data are expressed as the mean±SD. Otherwise, the Mann-Whitney U test was used, and the data are expressed as the median (IQR). For categorical characteristics, the $\chi^2$ test or Fisher's exact test was used, and these data are expressed as counts (%). A binary logistic regression model was used to analyse QCT features associated with RP-ILD. Survival outcomes were calculated using the Kaplan-Meier method and compared using the log-rank test. Variables identified as significant in univariate Cox proportional-hazards regression analysis were integrated into a multivariate Cox proportional-hazards regression model. The concordance index (C-index) was applied to evaluate the performance of the survival analysis models.[28] Mediation analysis was conducted to investigate the mediating effects of variables between independent and dependent variables.[29] A two-sided p value <0.05 defined statistical significance.

### Patient and public involvement

Due to the observational nature of this study, which used existing clinical data, patients were not directly involved in the initial research stages, such as question formulation or study design. The research focus and outcome

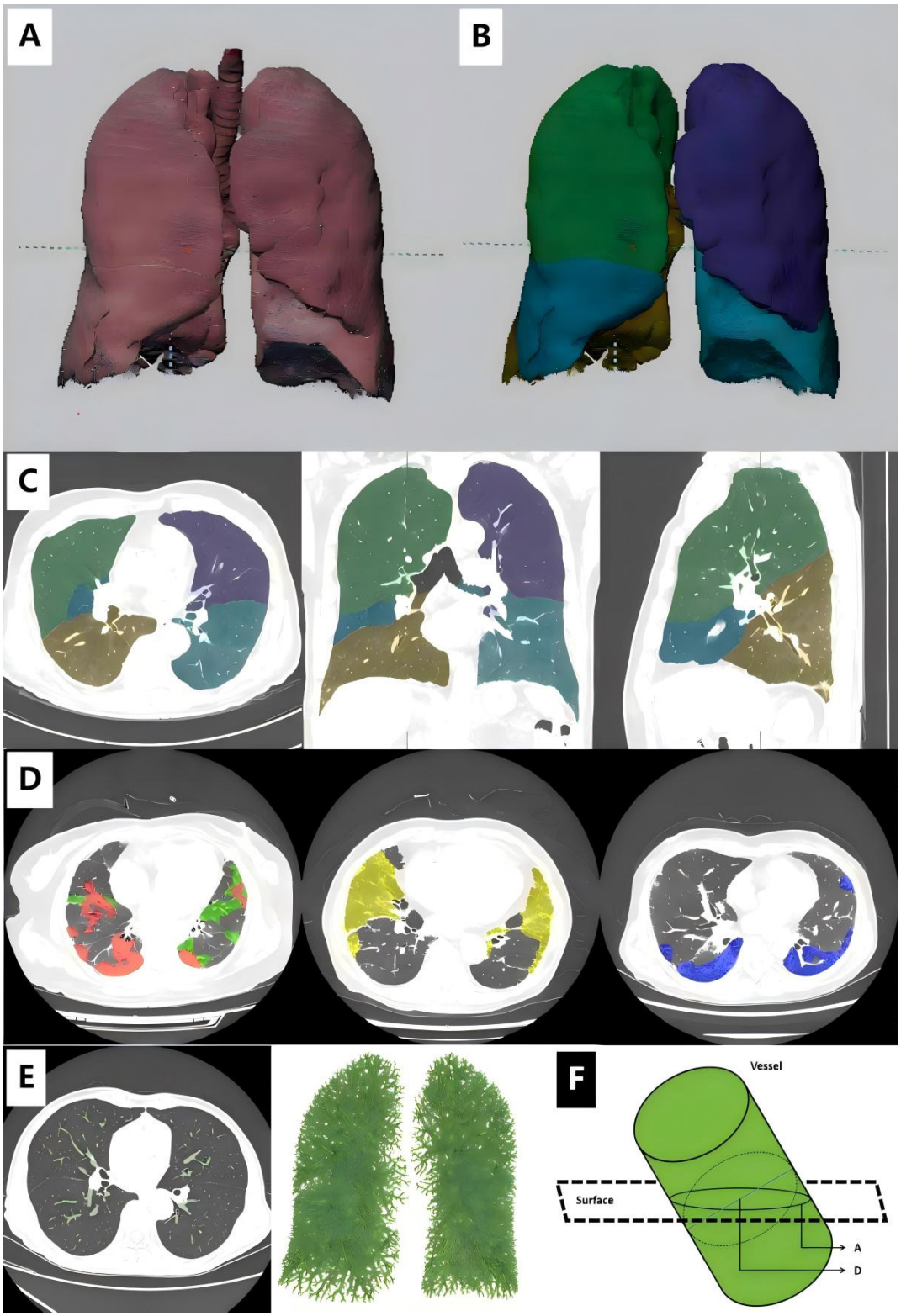


**Figure 2** Segmentation and schematic diagram of pulmonary vessel-related structures. (A) Automated segmentation of the entire lungs using a 3D-UNet-based model. (B) Three-dimensional schematic representation of automatically segmented lung lobes. (C) Multiplanar visualisation of lung lobe segmentation: axial, sagittal and coronal views. (D) Segmentation of interstitial lung disease imaging features: red—consolidation; green—ground-glass opacity; yellow—honeycombing; blue—reticular pattern. (E) The pulmonary blood vessels are automatically segmented using a 3D-UNet-based segmentation model and calculated using a three-dimensional quantitative algorithm. (F) A=area and D=diameter. The 'Surface' is the cross-section of HRCT and pulmonary blood vessels, the 'Area' represents the area of the cross-section of the pulmonary vessels. When combined with 3D reconstruction, the 'Diameter' of blood vessels can be calculated. The density is the average CT value of the entire vascular structure. HRCT, high-resolution computed tomography.

measures, including mortality and disease progression, were chosen based on their clinical relevance and importance to patients with IIM-ILD. As the study relied solely on routinely collected medical data, no additional burden was placed on participants. We are committed to sharing the study results with the patient community. Key findings will be summarised in plain language and disseminated through patient support groups and clinical departments to support better disease understanding and care.

## RESULTS

### Clinical characteristics

As shown in figure 1, 514 patients diagnosed with IIM-ILD (367 females; median age, 54 years) at our hospital were initially included, of which 249 cases (165 females; median age, 55 years) were identified as suffering from RP-ILD. Table 1 presents the clinical and demographic data for the patients. Notably, RP-ILD patients exhibited a higher prevalence of anti-MDA5 antibody positivity compared with those with non-RP-ILD. Additionally, they demonstrated reduced lung volumes, ventilation and gas exchange capabilities and decreased arterial oxygen partial pressure. Furthermore, RP-ILD patients showed more pronounced emphysema and interstitial lesions, along with elevated levels of creatine kinase, serum ferritin, lactate dehydrogenase (LDH) and alanine aminotransferase.

Meanwhile, an independent external cohort of 64 IIM-ILD patients (43 females; median age, 54 years) was enrolled from the second hospital, comprising 44 patients with ASS and 20 patients with MDA5+DM. As detailed in online supplemental table 1, the baseline characteristics of this external cohort showed no significant differences from those of the training cohort.

### PVRS and rapid progression of IIM-ILD

Multivariable analysis, adjusted for age, sex, height and weight, revealed that several PVRS parameters remained significantly associated with rapid progression of IIM-ILD (online supplemental table 2). An increased mean pulmonary vascular diameter (mPVD) was independently associated with a higher risk of RP-ILD, with the strength of association being inversely related to the distance from the pleura. The adjusted ORs were 5.30 (95% CI 2.74 to 10.23) at 6 mm, 4.26 (95% CI 2.13 to 8.53) at 9 mm and 2.75 (95% CI 1.27 to 5.99) at 12 mm. Similarly, an elevated standard deviation of the pulmonary vascular diameter (sdPVD) was an independent factor associated with the outcome across various distances from the pleura (OR range: 2.14–12.88; figure 3). Furthermore, greater total pulmonary vascular volume also conferred an increased risk of RP-ILD (OR 1.36, 95% CI: 1.23 to 1.50). These associations were consistently observed in patients with ASS (online supplemental table 3). In contrast, among patients with MDA5+DM, the effects were primarily evident in vessels nearer to the pleural surface (online supplemental table 4).

### Risk factors for poor prognosis of IIM-ILD patients

The follow-up period for our study concluded in June 2024, during which time the outcomes of 392 patients were definitively determined, while 122 patients were lost to follow-up (online supplemental table 5). The median follow-up duration, calculated using the reverse Kaplan-Meier method, was 9.67 years (95% CI 8.26 to 12.42), representing time from disease onset to the final outcome rather than from study enrolment, as numerous patients experienced disease onset prior to registry accrual.

Among those with a definitive prognosis, three experienced poor outcomes (one mortality, two ICU admissions) due to the involvement of systems other than the lungs prior to the onset of respiratory symptoms. Composite poor outcomes were defined as mortality, ICU admission or lung transplantation. The prognosis for RP-ILD and non-RP-ILD patients was notably distinct ($p<0.001$), as detailed in online supplemental table 6. The non-RP-ILD group exhibited excellent survival rates: 99.5% at 3 months, 99.0% at 6 months, 98.5% at 1 year and 97.4% at 2 years. In stark contrast, the RP-ILD group had substantially lower survival rates: 86.4% at both 3 and 6 months, 80.1% at 1 year and 77.4% at 2 years (online supplemental figure 1). As presented in table 2, age (HR 1.03, 95% CI 1.01 to 1.06), GGO% (HR 1.04, 95% CI 1.02 to 1.06) and the sdPVD at 6 mm (HR 1.25, 95% CI 1.02 to 1.54) and the sdPVD at 18 mm (HR 1.35, 95% CI 1.12 to 1.63) from the pleura on HRCT were independent risk factors for poor prognosis in ASS patients. The model incorporating these factors demonstrated moderate accuracy (C-index=0.819). For patients with MDA5+DM, age (HR 1.06, 95% CI 1.02 to 1.11), the mPVD at 6 mm from the pleura (HR 1.37, 95% CI 1.11 to 1.70) and LDH (HR 1.01, 95% CI 1.01 to 1.01) were independent risk factors for poor prognosis. The C-index for this model is 0.835, also indicating accuracy above the medium threshold.

Based on Cox regression analysis, the optimal cut-off values for prognostic stratification were determined as follows: 2.38 mm for mPVD at 6 mm from the pleura, 1.50 mm for sdPVD at 6 mm and 1.92 mm for sdPVD at 18 mm (online supplemental figure 2). Group comparisons using these thresholds revealed significant clinical differences. Among patients with MDA5+DM, those with an mPVD exceeding 2.38 mm had significantly lower $FEV_1$%, more extensive interstitial lesions and higher LDH levels (online supplemental table 7). Similarly, in the ASS group, patients with an sdPVD above the cut-off values exhibited worse lung volumes, impaired ventilatory function, greater interstitial involvement and elevated levels of C reactive protein and LDH (online supplemental tables 8 and 9).

The mediating effect analysis provides important insights into the pathways through which specific

**Table 1** Characteristics of included patients with idiopathic inflammatory myopathy*

| Characteristics | Non-RP-ILD | RP-ILD | P value |
|---|---|---|---|
| n | 265 | 249 | |
| Subtype, n (%) | | | **<0.001** |
| ASS | 211 (41.05%) | 146 (28.40%) | |
| MDA5+DM | 54 (10.51%) | 103 (20.04%) | |
| Female, n (%) | 202 (39.30%) | 165 (32.10%) | **0.013** |
| Age, median (IQR) | 54.00 (46.00, 60.00) | 55.00 (47.50, 63.00) | **0.043** |
| BMI, median (IQR) | 23.75 (21.50, 26.25) | 24.37 (22.59, 26.19) | 0.102 |
| Smoke, n (%) | | | **0.005** |
| Current | 3 (2.63) | 6 (9.52) | |
| Former | 3 (2.63) | 7 (11.11) | |
| Never | 108 (94.74) | 50 (79.37) | |
| Duration of the disease (months), median (IQR) | 4.50 (1.17, 17.53) | 3.13 (1.38, 11.73) | 0.286 |
| VC%, median (IQR) | 76.65 (64.775, 89.45) | 68.40 (57.10, 79.00) | **0.003** |
| FVC%, median (IQR) | 77.95 (65.40, 91.08) | 69.65 (56.33, 81.55) | **<0.001** |
| $FEV_1$%, median (IQR) | 76.10 (63.10, 86.88) | 67.45 (55.925, 79.75) | **0.002** |
| $FEV_1$/FVC%, median (IQR) | 80.55 (76.368, 84.86) | 81.28 (77.02, 86.15) | **<0.001** |
| TLC%, median (IQR) | 73.3 (62.95, 83.25) | 65.35 (54.83, 77.65) | **0.002** |
| $DL_{CO}$ SB%, median (IQR) | 61.70 (51.05, 71.65) | 50.55 (43.15, 60.28) | **<0.001** |
| $PaO_2$, median (IQR) | 87.60 (80.00, 95.00) | 80.25 (71.43, 91.65) | **0.006** |
| $PaCO_2$, median (IQR) | 37.90 (35.20, 40.80) | 36.45 (33.70, 39.78) | **<0.001** |
| The time from respiratory symptom onset to treatment initiation (month), median (IQR) | 0.82 (0.00, 4.04) | 0.88 (0.00, 2.36) | 0.971 |
| Initial treatment strategy, n (%) | | | **<0.001** |
| Glucocorticoid | 85 (40.09) | 76 (36.71) | |
| Glucocorticoid + immunosuppressant (dual) | 100 (47.17) | 74 (35.75) | |
| Glucocorticoid + immunosuppressants (triple combination) | 6 (2.83) | 4 (1.93) | |
| Glucocorticoid + immunoglobulin | 3 (1.42) | 14 (6.76) | |
| Glucocorticoid + immunosuppressant(s) + immunoglobulin | 18 (8.49) | 37 (17.87) | |
| Glucocorticoid + biologics | 0 (0.00) | 2 (0.97) | |
| Initial antifibrotic therapy, n (%) | 16 (7.55) | 10 (4.78) | 0.239 |
| Emphysema%, median (IQR) | 0.05 (0.02, 0.19) | 0.09 (0.03, 0.31) | **<0.001** |
| Consolidation%, median (IQR) | 0.13 (0.04, 0.39) | 0.27 (0.10, 0.59) | **<0.001** |
| Ground glass opacity%, median (IQR) | 2.46 (0.79, 7.29) | 5.42 (1.41, 14.68) | **<0.001** |
| Reticular pattern%, median (IQR) | 3.03 (1.22, 5.90) | 5.01 (2.25, 9.38) | **<0.001** |
| Honeycomb%, median (IQR) | 0.02 (0.00, 0.07) | 0.05 (0.01, 0.19) | **<0.001** |
| CK (IU/L), median (IQR) | 62.00 (33.00, 174.50) | 50.00 (27.00, 136.00) | **0.045** |
| CRP (mg/L), median (IQR) | 0.38 (0.21, 0.98) | 0.46 (0.26, 1.01) | 0.228 |
| ESR (mm/h), median (IQR) | 16.00 (8.50, 28.00) | 17.50 (9.00, 30.00) | 0.321 |
| Fet (ng/mL), median (IQR) | 151.85 (60.43, 369.35) | 359.10 (109.85, 943.45) | **<0.001** |
| LDH (IU/L), median (IQR) | 252.00 (197.00, 321.50) | 282.00 (229.00, 355.50) | **<0.001** |
| ALT (IU/L), median (IQR) | 27.50 (17.25, 47.75) | 34.00 (22.00, 59.00) | **0.002** |
| AST (IU/L), median (IQR) | 23.50 (17.00, 37.00) | 26.00 (18.00, 45.00) | 0.061 |

*Bold values indicate statistical significance at P<0.05.
ALT, alanine aminotransferase; ASS, antisynthetase syndrome; AST, aspartate aminotransferase; BMI, body mass index; CRP, C reactive protein; $DL_{CO}$SB%, the proportion of actual value to the expected value for carbon monoxide diffusing capacity,; ESR, erythrocyte sedimentation rate; Fet, ferritin; $FEV_1$%, the proportion of actual value to the expected value for forced expiratory volume in the first second; $FEV_1$/FVC, the proportion of forced expiratory volume in the first second to the forced vital capacity; $FiO_2$, fraction of inhaled oxygen; FVC%, the proportion of actual value to the expected value for forced vital capacity; LDH, lactic dehydrogenase; MDA5+DM, antimelanoma differentiation-associated gene 5 antibody-positive dermatomyositis; $PaCO_2$, arterial carbon dioxide pressure; $PaO_2$, arterial oxygen pressure; RP-ILD, rapidly progressive interstitial lung disease; TLC%, the proportion of actual value to the expected value for total lung capacity; VC%, the proportion of actual value to the expected value for vital capacity.

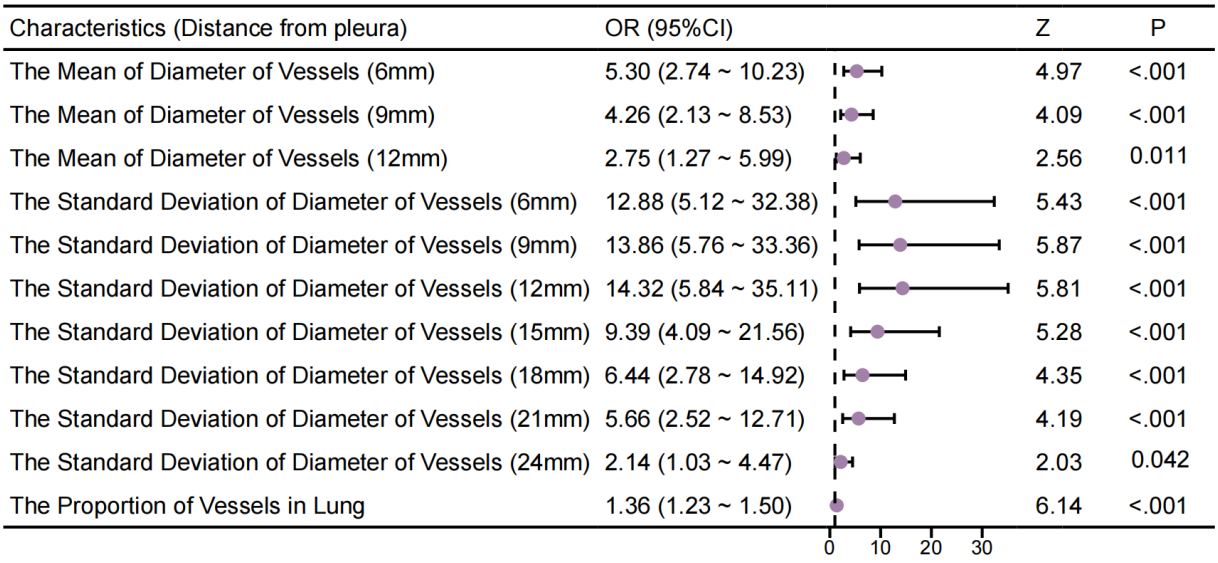


**Figure 3** Effect of pulmonary vessel diameter and volume on the rapid progression of IIM-ILD. IIM-ILD, idiopathic inflammatory myopathy-related interstitial lung disease. The unit of diameter is mm, and the unit of volume proportion is %*100.

variables influence the prognosis of patients with MDA5+DM ILD and ASS-ILD. In MDA5+DM patients, mPVD measured 6 mm from the pleura was found to have a direct impact on patient prognosis. Additionally, the mPVD exerted an indirect negative impact on prognosis through LDH as an intermediary factor (online supplemental table 10). In ASS patients, the results were somewhat different (online supplemental tables 11 and 12). The indirect and mediating effects of GGO% were significant, while other variables did not show significant indirect and mediating effects (online supplemental tables 11 and 12). This

**Table 2** Multivariate Cox proportional risk regression analysis of long-term survival in patients with antisynthetase syndrome and antimelanoma differentiation-associated gene 5 antibody-positive dermatomyositis*

| Variables | β | SE | Z | P value | HR (95% CI) |
|---|---|---|---|---|---|
| Antisynthetase syndrome | | | | | |
| Age | 0.03 | 0.01 | 2.37 | 0.018 | 1.03 (1.01 to 1.06) |
| GGO% | 0.04 | 0.01 | 4.17 | <0.001 | 1.04 (1.02 to 1.06) |
| The SD of diameter of vessels (6 mm) (dmm) | 0.22 | 0.10 | 2.16 | 0.031 | 1.25 (1.02 to 1.54) |
| The SD of diameter of vessels (18 mm) (dmm) | 0.30 | 0.10 | 3.11 | 0.002 | 1.35 (1.12 to 1.63) |
| The SD of diameter of vessels (21 mm) (dmm) | −0.15 | 0.08 | −1.95 | 0.051 | 0.86 (0.74 to 1.00) |
| Antimelanoma differentiation-associated gene 5 antibody-positive dermatomyositis | | | | | |
| Age | 0.06 | 0.02 | 2.79 | 0.005 | 1.06 (1.02 to 1.11) |
| The mean of diameter of vessels (6 mm) (dmm) | 0.32 | 0.11 | 2.97 | 0.003 | 1.37 (1.11 to 1.70) |
| The SD of diameter of vessels (12 mm) (dmm) | −0.24 | 0.15 | −1.63 | 0.103 | 0.78 (0.58 to 1.05) |
| Fet | −0.00 | 0.00 | −1.86 | 0.063 | 1.00 (1.00 to 1.00) |
| LDH | 0.01 | 0.00 | 3.09 | 0.002 | 1.01 (1.01 to 1.01) |
| AST | 0.00 | 0.00 | 1.81 | 0.071 | 1.00 (1.00 to 1.00) |

*The vascular-related independent variable is expressed as variables (distance from the pleura).
AST, aspartate aminotransferase; Fet, ferritin; GGO, ground glass opacity; LDH, lactic dehydrogenase.

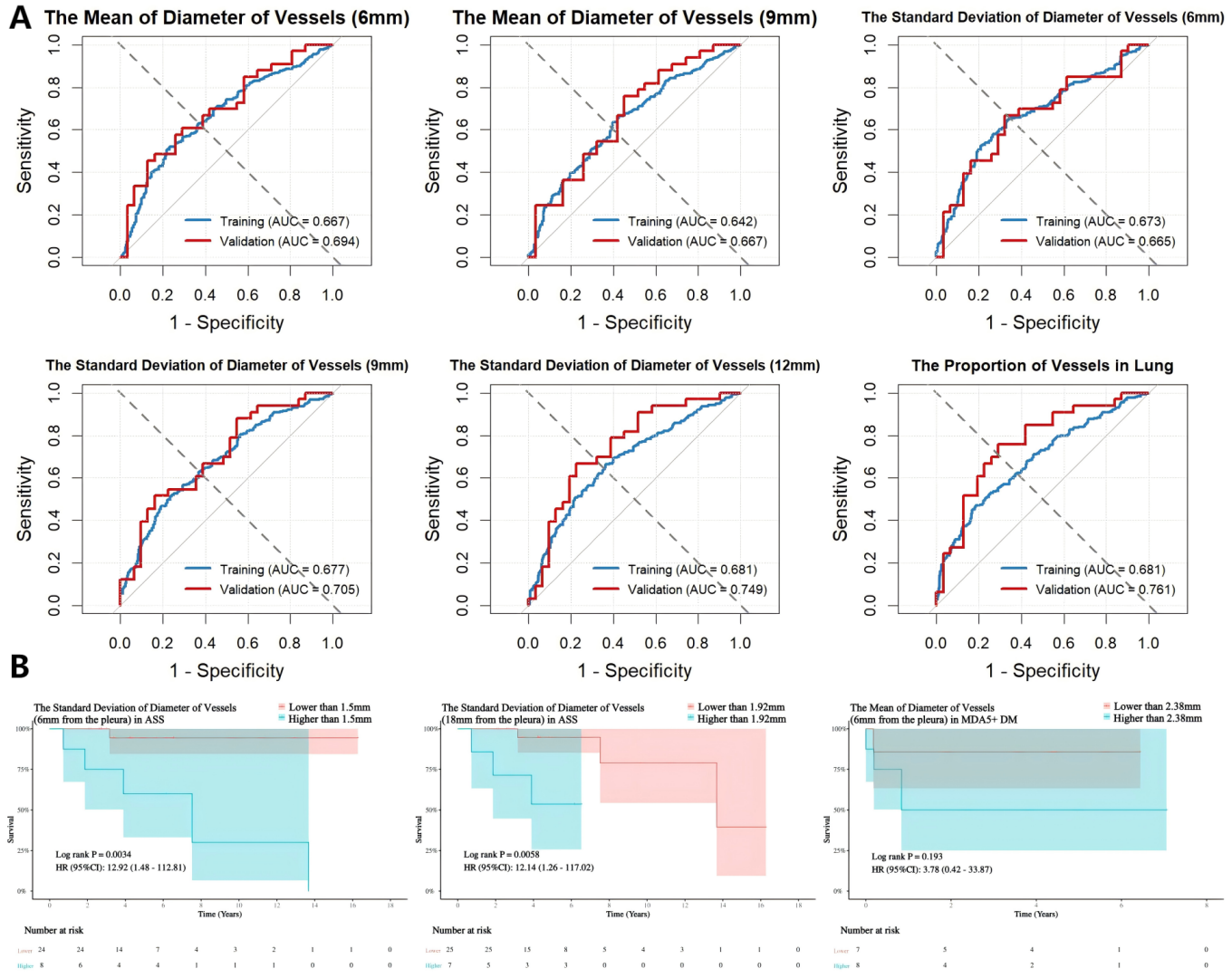


**Figure 4** ROC curves of PVRS for predicting RP-ILD and Kaplan-Meier curves stratified by the Cox regression cut-off value in the exterior validation cohort. ASS, anti-synthetase syndrome; AUC, area under the receiver operating characteristic curve; MDA5+DM, anti-melanoma differentiation-associated gene five antibody-positive dermatomyositis; PVRS, pulmonary vessel related structures; ROC, receiver operating characteristic; RP-ILD, rapid progressive interstitial lung disease.

indicates that the sdPVD (measured 6 mm and 18 mm from the pleura) directly affects prognosis and indirectly influences it negatively through GGO% as an intermediary factor.

## External validation

As illustrated in figure 4A, the discriminatory ability of PVRS parameters for RP-ILD in the external validation cohort from the second hospital was consistent with that in the internal training cohort from the first hospital. When the multivariate Cox regression model developed in the internal training cohort was applied to the external validation cohort of patients with ASS-ILD, the C-index for composite poor outcomes was 0.841, compared with 0.819 in the internal cohort. For MDA5+DM ILD, the C-index was 0.814, closely matching the internal value of 0.835. Furthermore, calibration curves (online supplemental figure 3) show the close alignment between the observed outcomes, indicating that the PVRS parameters are well-calibrated and provide reliable risk estimates for RP-ILD in both ASS-ILD and MDA5+DM ILD patients.

As summarised in online supplemental table 13, stratification based on PVRS cut-off values in the external cohort revealed significant differences. ASS patients with greater vascular diameter dispersion at 6 mm from the pleura exhibited worse ventilatory and gas exchange functions, as well as more extensive GGO and reticular patterns. Those with greater vascular diameter dispersion at 18 mm from the pleura showed reduced diffusion capacity and broader inflammatory lesions. MDA5+DM patients with wider vascular diameters at 6 mm from the pleura had more extensive GGO. Kaplan-Meier analysis (figure 4B) demonstrated that survival curves stratified by PVRS cut-off values remained significantly distinct in the external validation cohort.

## DISCUSSION

IIM represents a heterogeneous group of diseases, with ILD being a well-established, major pulmonary complication that significantly influences morbidity and mortality. Recent studies have extensively characterised the CT features and clinical outcomes of IIM-ILD.[30 31] Building on this critical foundation, our two-centre study provides the first evidence that PVRS derived from AI-based QCT, particularly the mPVD and sdPVD, is an independent risk factor for rapid progression in both ASS-ILD and MDA5+DM ILD, offering a novel perspective beyond parenchymal assessment.

In the RP-ILD group, a reduced number of pulmonary vessels was observed, along with a higher mean and SD of vessel intensity compared with the non-RP-ILD group. Furthermore, age, GGO% and sdPVD at different subpleural distances (6 mm and 18 mm) were identified as significant risk factors for poor prognosis in patients with ASS. In patients with MDA5+DM, age, mean subpleural vascular diameter at 6 mm and LDH level were key prognostic factors. Further analysis revealed the direct effects of these PVRS on patient outcomes, as well as indirect effects mediated by LDH (in MDA5+DM) and GGO% (in ASS).

While the existing paradigm of IIM-ILD[30 31] rightly focuses on parenchymal patterns like GGO, our findings underscore that concomitant pulmonary vascular remodelling is a critical and measurable phenotype. This vascular component may act independently or synergistically with the interstitial process to drive disease progression, thereby proposing a more comprehensive, dual-pathway (vascular and interstitial) model for understanding and stratifying IIM-ILD.

Currently, the emergence of QCT with AI technologies, leveraging CT data, has marked a transformative shift in the approach to objectively and efficiently studying diseases.[32–36] Our findings indicate that in the RP-ILD group, AI-based QCT revealed a reduced number of pulmonary vessels and a high degree of sdPVD and SD of vascular intensity, which may reflect the uneven impairment of the vascular bed in conjunction with interstitial destruction—a pathognomonic feature of ILD characterised by extensive parenchymal and interstitial damage leading to pulmonary vascular bed loss.[11]

The expansion of PVRS volume likely stems from multifaceted vascular remodelling mechanisms. Pathological thickening of vascular walls arises from endothelial cell proliferation, smooth muscle cell hypertrophy and extracellular collagen deposition, while aberrant angiogenesis disrupts normal vascular architecture and haemodynamics.[37] Concomitantly, inflammatory infiltration and fibrotic transformation impair alveolar-capillary gas exchange, establishing a hypoxic microenvironment that triggers compensatory neovascularisation to meet heightened metabolic demands.[18 38 39] Persistent hypoxia triggers hypoxic pulmonary vasoconstriction that drives shear stress-associated vascular remodelling, manifested as proliferation and hypertrophy of vascular smooth muscle cells.[40] Additionally, hypoxia activates inflammation, releases a large number of pro-angiogenic factors, induces pathological vascular remodelling and aggravates pulmonary vascular injury.[41–43]

Studies have demonstrated the occurrence of vascular remodelling in IPF,[44–49] a process that is particularly pronounced in regions adjacent to fibroblast lesions, and the blood vessel density within the fibroblast lesions is reduced.[44] This biphasic pattern of vascular remodelling is further characterised by temporally dynamic angiogenic responses: the dynamic of angiogenesis in pulmonary fibrosis initially exhibits an upsurge, peaking at a certain point, before subsequently diminishing to levels below normalcy. During the initial phase of microfibrosis development, there is an increase in capillary density. Conversely, in areas with advanced fibrosis, capillary density diminishes. Importantly, our imaging analyses corroborate this chronological trajectory, as heightened vascular intensity on QCT—likely reflecting the hyperproliferative phase—showed strong association with rapid disease progression.

In patients with MDA5+DM, LDH emerges as a direct risk factor and a mediator of subpleural vessel diameter, both of which impact patient prognosis. LDH itself usually does not have specific and direct ‘functional’ effects on blood vessels when it is released into the bloodstream. However, the underlying pathological conditions reflected by the release of LDH into the blood may affect blood vessels through inflammation-mediated pathophysiological mechanisms, enhanced oxidative stress and metabolic dysregulation. Inflammation-mediated vascular injury: serum LDH levels correlate with disease activity in IIM, reflecting myocyte damage and inflammatory responses. Inflammatory mediators (eg, cytokines) released during muscle injury directly impair vascular endothelial cells, leading to dysregulated vasodilation/constriction.[50–56] Oxidative stress mechanisms: LDH-driven glycolysis under hypoxia/inflammation promotes lactate accumulation and microenvironment acidification, exacerbating myocyte injury. Concurrent mitochondrial dysfunction generates excessive reactive oxygen species, damaging vascular smooth muscle cells and endothelial integrity via oxidative stress.[53 57–62] Metabolic dysregulation: chronic inflammation disrupts glucose/lipid metabolism via oxidative stress. Hyperglycaemia induces endothelial glycation, while dyslipidaemia promotes vascular lipid deposition, collectively accelerating atherosclerosis and vascular stenosis.[59 63–68]

Previous studies have demonstrated that PVRS stands as the most significant independent predictor of mortality in connective tissue disease-associated ILD patients.[18 69 70] Chung *et al*[19] revealed a negative correlation between PVRS and $DL_{CO}$% in connective tissue disease-associated ILD individuals. Our findings also indicate that the quantitative PVRS characteristics of vascular diameter directly affect the prognosis of patients. Consequently, quantitative pulmonary vascular CT features serve as a valuable tool for assessing disease severity and evaluating outcomes,

with PVRS emerging as a viable imaging marker in serial CT scans. Furthermore, QCT features offer insights into the quantity, volume, intensity and diameter of blood vessels, which, coupled with fundamental research, can deepen our understanding of the pathophysiological mechanisms underlying vascular alterations in ILD.

This is the first study to demonstrate that PVRS serves as a risk factor for RP-ILD and poor prognosis in patients with ASS and MDA5+DM; however, there are several limitations as follows: first, the sample size of our external validation cohort was relatively small, which may affect the generalisability of our findings and necessitate further confirmation in larger, multicentre studies. Second, potential biases inherent in the AI-based analysis should be considered. Spectrum bias may exist based on the composition and distribution of the training datasets used during its development. In addition, the accuracy of the segmentation is dependent on image quality and specific scanner protocols. Variations in these factors across institutions could affect the algorithm's performance when applied to new populations. Although it demonstrated high reproducibility in our internal validation, these potential biases suggest that its performance should be further validated across diverse clinical settings and equipment. Furthermore, the quantitative PVRS could not differentiate between arterial and venous vessels. Additionally, we failed to incorporate clinical features of pulmonary pressure from echocardiography or right heart catheterisation and did not thoroughly explore the relationship between PVRS and pulmonary arterial hypertension. Another limitation of this study is the 24% attrition rate, which may introduce selection bias. However, a comparison of baseline characteristics revealed that while there were differences in subtype, disease duration and ALT, the groups were comparable on key prognostic factors. Since our analysis was stratified by subtype and the other differing variables were not independent risk factors of the outcome, we believe the risk of substantial bias is low. Finally, during the inflammatory process, various cytokines and inflammatory mediators are produced. These inflammatory mediators can damage vascular endothelial cells, leading to their dysfunction, resulting in abnormal vasodilation and constriction functions of blood vessels. However, we did not analyse the correlation of PVRS with cytokines and inflammatory mediators.

## CONCLUSION

AI-based QCT enables the development of digital biomarkers that have significantly contributed to the assessment of prognosis and disease behaviour of IIM-ILD. The QCT features of PVRS at baseline in IIM-ILD patients were associated with rapid progression and were inversely associated with interstitial lesions and pulmonary function outcomes. Quantitative characteristics of pulmonary vessel diameter are risk factors for poor prognosis in patients with IIM-ILD.

**Author affiliations**
[1]Immune Dysfunction and Pulmonary Fibrosis Joint Laboratory for Clinical Medicine, Capital Medical University, Beijing, China
[2]National Center for Respiratory Medicine; State Key Laboratory of Respiratory Health and Multimorbidity; National Clinical Research Center for Respiratory Diseases; Institute of Respiratory Medicine, Chinese Academy of Medical Sciences; Department of Pulmonary and Critical Care Medicine, Center of Respiratory Medicine, China-Japan Friendship Hospital, Beijing, China
[3]China-Japan Friendship Hospital (Institute of Clinical Medical Sciences), Chinese Academy of Medical Sciences & Peking Union Medical College, Beijing, China
[4]Department of Pulmonary and Critical Care Medicine, General Hospital of Ningxia Medical University, Yinchuan, China
[5]Department of Radiology, China-Japan Friendship Hospital, Beijing, China
[6]Department of Radiology, General Hospital of Ningxia Medical University, Yinchuan, China

**Contributors** Conception and design: ML and HD. Administrative support: HD. Provision of study materials or patients: YH, YR, BX, SW, LZ, JG and HD. Collection and assembly of data: YQ, HW, XY, YN, JW, AL, JD, YH, YR, BX, SW, LZ and JG. Data analysis and interpretation: YQ, HW, XY, ML and HD. Manuscript writing: YQ, HW and XY. Revision: YQ, HW, XY, ML and HD. Final approval of manuscript: all authors. The guarantor: Huaping Dai. HRCT images in the Digital Imaging and Communications in Medicine format were transferred to an in-house AI workstation (CT quantitative system: SIMBIO-T, Hangzhou Smart Intelligent Technology Hangzhou, China) for automatic quantitative analysis of lung parenchyma, pulmonary vessels, lung texture and radiomics parameters. The analysis pipeline consisted of two main phases (figure 2): (1) AI-based segmentation and quantification. The commercial AI algorithm was applied to automatically segment the entire lung, its lobes, pulmonary vessels and interstitial lesions and to calculate various quantitative features related to these structures. Prior to its use in this study, the performance of this algorithm was independently validated by our team on a subset of our dataset that was not included in the final analysis. Segmentation accuracy was assessed by quantifying the agreement between the AI output and manual annotations made by an expert radiologist using the Dice similarity coefficient (DSC), which was 0.95±0.02. The reproducibility of quantitative measurements was evaluated using the intraclass correlation coefficient (ICC), which was 0.92. (2) Radiologist review and adjudication: two chest radiologists with 9 and 15 years of experience independently evaluated all AI-generated segmentations using a standardised scoring system. Both radiologists were blinded to clinical information and to each other's assessments. Any discrepancies in the evaluations were resolved through a consensus discussion with a third senior chest radiologist with 22 years of experience.

**Funding** This study was supported by the National Key Technologies R & D Program Precision Medicine Research (Nos. 2021YFC2500700 and 2016YFC0901101) and the National Natural Science Foundation of China (No. 81870056).

**Competing interests** None declared.

**Patient and public involvement** Patients and/or the public were not involved in the design, conduct, reporting or dissemination plans of this research.

**Patient consent for publication** Consent obtained directly from patient(s).

**Ethics approval** This study involves human participants. This study was conducted in accordance with the ethical standards of the institutional ethics committee and the Helsinki Declaration of 1975 (as revised in 2000). The institutional ethics committee of China-Japan Friendship Hospital approved the study protocol on 1 January 2019 (approval no. KYLL-2019-455). The Institutional Ethics Committee of General Hospital of Ningxia Medical University approved the study protocol on 16 March 2017 (approval no. 2017-25). Informed consent was obtained from all participants. Participants gave informed consent to participate in the study before taking part.

**Provenance and peer review** Not commissioned; externally peer reviewed.

**Data availability statement** Data are available upon reasonable request.

**ORCID iDs**
Yuhui Qiang https://orcid.org/0009-0001-1403-1559
Linfeng Xi https://orcid.org/0000-0001-5702-4159
Shiyao Wang https://orcid.org/0000-0002-1066-4850
Min Liu https://orcid.org/0000-0003-1298-4441

## REFERENCES

1 Douglas WW, Tazelaar HD, Hartman TE, *et al*. Polymyositis–Dermatomyositis-associated Interstitial Lung Disease. *Am J Respir Crit Care Med* 2001;164:1182–5.
2 Schmidt J. Current Classification and Management of Inflammatory Myopathies. *J Neuromuscul Dis* 2018;5:109–29.
3 Betteridge Z, McHugh N. Myositis-specific autoantibodies: an important tool to support diagnosis of myositis. *J Intern Med* 2016;280:8–23.
4 Lia Y, Fana Y, Wanga Y, *et al*. Phenotypic clusters and survival analyses in interstitial pneumonia with myositis-specific autoantibodies. *Sarcoidosis Vasc Diffuse Lung Dis* 2022;38:e2021047.
5 Pinal-Fernandez I, Casal-Dominguez M, Mammen AL. Immune-Mediated Necrotizing Myopathy. *Curr Rheumatol Rep* 2018;20:21.
6 Shi J, Li S, Yang H, *et al*. Clinical Profiles and Prognosis of Patients with Distinct Antisynthetase Autoantibodies. *J Rheumatol* 2017;44:1051–7.
7 Hamaguchi Y, Fujimoto M, Matsushita T, *et al*. Common and Distinct Clinical Features in Adult Patients with Anti-Aminoacyl-tRNA Synthetase Antibodies: Heterogeneity within the Syndrome. *PLoS ONE* 2013;8:e60442.
8 Zuo Y, Ye L, Chen F, *et al*. Different Multivariable Risk Factors for Rapid Progressive Interstitial Lung Disease in Anti-MDA5 Positive Dermatomyositis and Anti-Synthetase Syndrome. *Front Immunol* 2022;13:845988.
9 Raghu G, Remy-Jardin M, Richeldi L, *et al*. Idiopathic Pulmonary Fibrosis (an Update) and Progressive Pulmonary Fibrosis in Adults: An Official ATS/ERS/JRS/ALAT Clinical Practice Guideline. *Am J Respir Crit Care Med* 2022;205:e18–47.
10 Won Huh J, Soon Kim D, Keun Lee C, *et al*. Two distinct clinical types of interstitial lung disease associated with polymyositis-dermatomyositis. *Respir Med* 2007;101:1761–9.
11 Jacob J, Bartholmai BJ, Rajagopalan S, *et al*. Mortality prediction in idiopathic pulmonary fibrosis: evaluation of computer-based CT analysis with conventional severity measures. *Eur Respir J* 2017;49:1601011.
12 Clukers J, Lanclus M, Mignot B, *et al*. Quantitative CT analysis using functional imaging is superior in describing disease progression in idiopathic pulmonary fibrosis compared to forced vital capacity. *Respir Res* 2018;19:213.
13 Yeo J, Yoon SH, Kim JY, *et al*. Quantitative interstitial lung disease scores in idiopathic inflammatory myopathies: longitudinal changes and clinical implications. *Rheumatology (Sunnyvale)* 2023;62:3690–9.
14 Handa T, Tanizawa K, Oguma T, *et al*. Novel Artificial Intelligence-based Technology for Chest Computed Tomography Analysis of Idiopathic Pulmonary Fibrosis. *Annals ATS* 2022;19:399–406.
15 Jacob J, Bartholmai BJ, Rajagopalan S, *et al*. Unclassifiable-interstitial lung disease: Outcome prediction using CT and functional indices. *Respir Med* 2017;130:43–51.
16 Jacob J, Bartholmai BJ, Rajagopalan S, *et al*. Predicting Outcomes in Idiopathic Pulmonary Fibrosis Using Automated Computed Tomographic Analysis. *Am J Respir Crit Care Med* 2018;198:767–76.
17 Jacob J, Bartholmai BJ, Egashira R, *et al*. Chronic hypersensitivity pneumonitis: identification of key prognostic determinants using automated CT analysis. *BMC Pulm Med* 2017;17:81.
18 Chung JH, Adegunsoye A, Oldham JM, *et al*. Vessel-related structures predict UIP pathology in those with a non-IPF pattern on CT. *Eur Radiol* 2021;31:7295–302.
19 Chung JH, Adegunsoye A, Cannon B, *et al*. Differentiation of Idiopathic Pulmonary Fibrosis from Connective Tissue Disease-Related Interstitial Lung Disease Using Quantitative Imaging. *JCM* 2021;10:2663.
20 Jacob J, Bartholmai BJ, Brun AL, *et al*. Evaluation of visual and computer-based CT analysis for the identification of functional patterns of obstruction and restriction in hypersensitivity pneumonitis. *Respirology* 2017;22:1585–91.
21 Travis WD, Costabel U, Hansell DM, *et al*. An Official American Thoracic Society/European Respiratory Society Statement: Update of the International Multidisciplinary Classification of the Idiopathic Interstitial Pneumonias. *Am J Respir Crit Care Med* 2013;188:733–48.
22 Mathai SC, Danoff SK. Management of interstitial lung disease associated with connective tissue disease. *BMJ* 2016;352:h6819.
23 Mammen AL, Allenbach Y, Stenzel W, *et al*. 239th ENMC International Workshop: Classification of dermatomyositis, Amsterdam, the Netherlands, 14-16 December 2018. *Neuromuscul Disord* 2020;30:70–92.
24 Bohan A, Peter JB. Polymyositis and dermatomyositis(first of two parts). *N Engl J Med* 1975.
25 Cavagna L, Trallero-Araguás E, Meloni F, *et al*. Influence of Antisynthetase Antibodies Specificities on Antisynthetase Syndrome Clinical Spectrum Time Course. *JCM* 2019;8:2013.
26 Ye S, Chen X, Lu X, *et al*. Adult clinically amyopathic dermatomyositis with rapid progressive interstitial lung disease: a retrospective cohort study. *Clin Rheumatol* 2007;26:1647–54.
27 Xu L, You H, Wang L, *et al*. Identification of Three Different Phenotypes in Anti–Melanoma Differentiation–Associated Gene 5 Antibody–Positive Dermatomyositis Patients: Implications for Prediction of Rapidly Progressive Interstitial Lung Disease. *Arthritis & Rheumatology* 2023;75:609–19.
28 Harrell FE, Lee KL, Mark DB. MULTIVARIABLE PROGNOSTIC MODELS: ISSUES IN DEVELOPING MODELS, EVALUATING ASSUMPTIONS AND ADEQUACY, AND MEASURING AND REDUCING ERRORS. *Statist Med* 1996;15:361–87.
29 Baron RM, Kenny DA. The moderator-mediator variable distinction in social psychological research: Conceptual, strategic, and statistical considerations. *J Pers Soc Psychol* 1986;51:1173–82.
30 Karampitsakos T, Papaioannou O, Chrysikos S, *et al*. Clinical features and outcomes of patients with myositis associated-interstitial lung disease. ERS International Congress 2021 abstracts; September 5, 2021
31 Laporte A, Mariampillai K, Allenbach Y, *et al*. Idiopathic inflammatory myopathies: CT characteristics of interstitial lung disease and their association(s) with myositis-specific autoantibodies. *Eur Radiol* 2022;32:3480–9.
32 Xi L, Xu F, Kang H, *et al*. Clot ratio, new clot burden score with deep learning, correlates with the risk stratification of patients with acute pulmonary embolism. *Quant Imaging Med Surg* 2024;14:86–97.
33 Nurmohamed NS, Bom MJ, Jukema RA, *et al*. AI-Guided Quantitative Plaque Staging Predicts Long-Term Cardiovascular Outcomes in Patients at Risk for Atherosclerotic CVD. *JACC: Cardiovascular Imaging* 2024;17:269–80.
34 Felder FN, Walsh SLF. Exploring computer-based imaging analysis in interstitial lung disease: opportunities and challenges. *ERJ Open Res* 2023;9:00145–2023.
35 Trivedi AP, Hall C, Goss CW, *et al*. Quantitative CT Characteristics of Cluster Phenotypes in the Severe Asthma Research Program Cohorts. *Radiology* 2022;304:450–9.
36 Carini C, Seyhan AA. Tribulations and future opportunities for artificial intelligence in precision medicine. *J Transl Med* 2024;22:411.
37 Mondoni M, Rinaldo R, Ryerson CJ, *et al*. Vascular involvement in idiopathic pulmonary fibrosis. *ERJ Open Res* 2024;10:00550–2024.
38 Pugh CW, Ratcliffe PJ. Regulation of angiogenesis by hypoxia: role of the HIF system. *Nat Med* 2003;9:677–84.
39 Cosgrove GP, Brown KK, Schiemann WP, *et al*. Pigment epithelium-derived factor in idiopathic pulmonary fibrosis: a role in aberrant angiogenesis. *Am J Respir Crit Care Med* 2004;170:242–51.
40 Sakao S, Taraseviciene-Stewart L, Lee JD, *et al*. Initial apoptosis is followed by increased proliferation of apoptosis-resistant endothelial cells. *The FASEB Journal* 2005;19:1178–80.
41 Zhang Y, Li X, Li S, *et al*. Immunotherapy for Pulmonary Arterial Hypertension: From the Pathogenesis to Clinical Management. *IJMS* 2024;25:8427.
42 Wang R, Yuan T, Wang J, *et al*. Immunity and inflammation in pulmonary arterial hypertension: From pathophysiology mechanisms to treatment perspective. *Pharmacol Res* 2022;180:106238.
43 McLellan K, Papadopoulou C. Update on Biomarkers of Vasculopathy in Juvenile and Adult Myositis. *Curr Rheumatol Rep* 2022;24:227–37.
44 Renzoni EA, Walsh DA, Salmon M, *et al*. Interstitial Vascularity in Fibrosing Alveolitis. *Am J Respir Crit Care Med* 2003;167:438–43.

45 Leach HG, Chrobak I, Han R, *et al*. Endothelial Cells Recruit Macrophages and Contribute to a Fibrotic Milieu in Bleomycin Lung Injury. *Am J Respir Cell Mol Biol* 2013;49:1093–101.
46 Baruah J, Wary KK. Exosomes in the Regulation of Vascular Endothelial Cell Regeneration. *Front Cell Dev Biol* 2019;7:353.
47 Wu X, Gao Y, Xu L, *et al*. Exosomes from high glucose-treated glomerular endothelial cells trigger the epithelial-mesenchymal transition and dysfunction of podocytes. *Sci Rep* 2017;7:9371.
48 Muñoz-Espín D, Serrano M. Cellular senescence: from physiology to pathology. *Nat Rev Mol Cell Biol* 2014;15:482–96.
49 Xiong J, Kawagishi H, Yan Y, *et al*. A Metabolic Basis for Endothelial-to-Mesenchymal Transition. *Mol Cell* 2018;69:689–98.
50 Neves A, Mendonça I, Marques J, *et al*. Dermatomyositis and Crohn's disease – Case report. *Int J of Rheum Dis* 2023;26:2576–80.
51 Li W, Deng C, Yang H, *et al*. Upregulation of the CD155-CD226 Axis Is Associated With Muscle Inflammation and Disease Severity in Idiopathic Inflammatory Myopathies. *Neurol Neuroimmunol Neuroinflamm* 2023;10.
52 Banguera-Ordoñez YD, Sena-Torralba A, Quintero-Campos P, *et al*. Smartphone-based lateral flow immunoassay for sensitive determination of lactate dehydrogenase at the point of care. *Talanta* 2025;281:126803.
53 Mikołajczyk-Korona A, Dziedzic R, Wójcik K, *et al*. Enhanced systemic oxidative stress response in patients with idiopathic inflammatory myopathies. *Arthritis Res Ther* 2025;27:50.
54 Lemmer D, Schmidt J, Kummer K, *et al*. Impairment of muscular endothelial cell regeneration in dermatomyositis. *Front Neurol* 2022;13:952699.
55 Oh EK, Lee S-A, Lee HJ, *et al*. Clinical and Radiological Features of Korean Patients With Anti-HMGCR Myopathy. *J Clin Neurol* 2023;19:460.
56 Honda M, Shimizu F, Sato R, *et al*. Jo-1 Antibodies From Myositis Induce Complement-Dependent Cytotoxicity and TREM-1 Upregulation in Muscle Endothelial Cells. *Neurol Neuroimmunol Neuroinflamm* 2023;10.
57 Danieli MG, Antonelli E, Piga MA, *et al*. Oxidative stress, mitochondrial dysfunction, and respiratory chain enzyme defects in inflammatory myopathies. *Autoimmun Rev* 2023;22:103308.
58 Iacovino LG, Rossi M, Di Stefano G, *et al*. Allosteric transitions of rabbit skeletal muscle lactate dehydrogenase induced by pH-dependent dissociation of the tetrameric enzyme. *Biochimie* 2022;199:23–35.
59 Gupta GS. The Lactate and the Lactate Dehydrogenase in Inflammatory Diseases and Major Risk Factors in COVID-19 Patients. *Inflammation* 2022;45:2091–123.
60 Kumboyono K, Chomsy IN, Hakim AK, *et al*. Detection of Vascular Inflammation and Oxidative Stress by Cotinine in Smokers: Measured Through Interleukin-6 and Superoxide Dismutase. *Int J Gen Med* 2022;15:7319–28.
61 Chandrasekar B, Mummidi S, DeMarco VG, *et al*. Empagliflozin Reverses Oxidized LDL-Induced RECK Suppression, Cardiotrophin-1 Expression, MMP Activation, and Human Aortic Smooth Muscle Cell Proliferation and Migration. *Mediators Inflamm* 2023;2023:6112301.
62 Spitznagle JC, Kacha-Ochana A, Cook-Mills JM, *et al*. Increased vascular deposition of oxidized LDL in untreated juvenile dermatomyositis. *Pediatr Rheumatol Online J* 2024;22:73.
63 Shen J, San W, Zheng Y, *et al*. Different types of cell death in diabetic endothelial dysfunction. *Biomed Pharmacother* 2023;168:115802.
64 Wu WZ, Bai YP. Endothelial GLUTs and vascular biology. *Biomed Pharmacother* 2023;158:114151.
65 Shindo M, Maeda M, Myat K, *et al*. LDH-A—Modulation and the Variability of LDH Isoenzyme Profiles in Murine Gliomas: A Link with Metabolic and Growth Responses. *Cancers (Basel)* 2022;14:2303.
66 Gonzalez-Chapa JA, Macêdo MB, Lood C, *et al*. The Emerging Role of Mitochondrial Dysfunction in the Pathogenesis of Idiopathic Inflammatory Myopathies. *Rambam Maimonides Med J* 2023;14:e0006.
67 Zhao Q, Hu Q, Meng S, *et al*. Metabolic profiling of patients with different idiopathic inflammatory myopathy subtypes reveals potential biomarkers in plasma. *Clin Exp Med* 2023;23:3417–29.
68 Oreska S, Storkanova H, Pekacova A, *et al*. Cardiovascular risk in myositis patients compared with the general population. *Rheumatology (Oxford)* 2024;63:715–24.
69 Sadeghi S, Granton JT, Akhavan P, *et al*. Survival in rheumatoid arthritis-associated pulmonary arterial hypertension compared with idiopathic pulmonary arterial hypertension. *Respirology* 2015;20:481–7.
70 Takahashi K, Taniguchi H, Ando M, *et al*. Mean pulmonary arterial pressure as a prognostic indicator in connective tissue disease associated with interstitial lung disease: a retrospective cohort study. *BMC Pulm Med* 2016;16:55.